SQUID magnetometer operating at 37 K based on nanobridges in epitaxial MgB_2 thin films

D. Mijatovic, A. Brinkman,[a] D. Veldhuis, H. Hilgenkamp, H. Rogalla, G. Rijnders, and D. H. A. Blank
Faculty of Science and Technology and MESA+ Research Institute for Nanotechnology, University of Twente, P.O. Box 217, 7500 AE, Enschede, The Netherlands

A. V. Pogrebnyakov and J. M. Redwing
The Pennsylvania State University, Department of Materials Science and Engineering, University Park, Pennsylvania 16802

S. Y. Xu, Q. Li, and X. X. Xi
The Pennsylvania State University, Department of Physics, University Park, Pennsylvania 16802

(Received 10 June 2005; accepted 14 September 2005; published online 4 November 2005)

Superconducting quantum interference devices (SQUIDs) and magnetometers are fabricated from nanoconstrictions in epitaxial MgB_2 films. The nanobridges are contained within single-crystalline grains, resulting in clean transport, a large critical current density of 5×10^7 A/cm^2 at 4.2 K, and stable SQUID voltage modulation up to 38.8 K. The magnetometer is realized with an inductively coupled pickup loop, giving rise to a field sensitivity of 1 pT Hz$^{-1/2}$ down to 1 Hz. The device properties are governed by the two-band superconducting nature of MgB_2, posing, however, no problems to a successful development of boride magnetic field sensing devices. The MgB_2 zero-temperature London penetration depth is measured to be 62 nm, close to theoretical predictions. © *2005 American Institute of Physics*. [DOI: 10.1063/1.2128482]

The relatively large superconducting transition temperature of MgB_2 (T_c=39 K) and its metallic character make MgB_2 interesting for use in superconducting quantum interference devices (SQUIDs). MgB_2 would fill the existing gap between sensitive but low-T_c SQUIDs and the less-sensitive but high-T_c SQUIDs if high-quality magneto-sensing devices could be obtained that operate around 35 K and have good noise properties.

The first MgB_2 SQUID[1] was based on the principle that a nano-constriction with a size smaller than the London penetration depth can act as a weak link. Two nano-constrictions in a loop were focused ion beam etched in a pulsed laser deposited MgB_2 film, thereby forming a SQUID. Soon after, Zhang *et al.*[2] reported a MgB_2 SQUID based on tunable point contacts in polycrystalline bulk material. Although the method used is not very suitable for applications, the reported noise value for an optimally tuned SQUID ($\beta_L\sim1$) of 35 fT Hz$^{-1/2}$ above 500 Hz at 19 K is promising. Burnell *et al.*[3] realized MgB_2 SQUIDs operating up to 20 K by locally degrading the superconducting properties of MgB_2 through focused ion beam irradiation. The obtained voltage modulation is large and the white flux noise of 14 $\mu\Phi_0$ Hz$^{-1/2}$ is comparable to noise levels in high-T_c SQUIDs.

The operating temperature of all MgB_2 thin film SQUIDs reported so far, of about 20 K, is limited by the superconducting transition temperature of the films. In all cases, samples are considered that are polycrystalline and in the electronically dirty limit (scattering lengths are much smaller than device dimensions). It is to be expected that clean and single-crystalline thin films will be of importance in the step towards low-noise and highly reproducible devices. Here, we present the realization of SQUIDs in electronically clean, epitaxial MgB_2 with a high operating temperature. It is anticipated that in these crystalline structures, the multiband superconducting nature[4] of MgB_2 will influence the charge transport through the nano-constrictions.

Epitaxial MgB_2 films with T_c=40 K were obtained by hybrid physical-chemical Vapor deposition (HPCVD), as described in Ref. 5. The 100-nm-thick layers were deposited on 4H-SiC (5×5 mm^2) substrates at 718 °C. An increase in grain size was found with increasing B_2H_6 gas flow during deposition, from about 1.4 μm for samples prepared at 50 sccm B_2H_6 to about 2.2 μm for samples prepared at 150 sccm B_2H_6. The grain boundaries in MgB_2 act as strong links,[6,7] but even strong links can in principle still influence the critical current I_c in a nanobridge in an uncontrollable manner, something one would like to avoid in a SQUID. Here, we have the unique situation in which the dimensions of the nanobridges are much smaller than the grain size, thereby maximizing the chance for realizing a nanobridge within a single grain.

Coarse structures, such as the square-washer SQUID ring, the pickup loop and the contact leads were defined in the epitaxial films by standard photolithography and Ar ion-beam milling. Then, 100- or 140-nm-wide nanobridges were structured in 5-μm-wide predefined striplines by focused ion beam (FIB) etching, as described in Refs. 1 and 8. For some SQUIDs, prior to the film structuring, 25 nm of gold was deposited by rf sputter deposition to protect the film from degradation during structuring caused by the sensitivity of the MgB_2 to water.[9,10] During the nanobridge etching, gold is removed, to make sure that the electrical transport through the bridges is not influenced by this capping layer. The electrical transport properties of the devices were measured in a shielded variable-temperature cryostat.

[a]Author to whom correspondence should be addressed; electronic mail: a.brinkman@utwente.nl

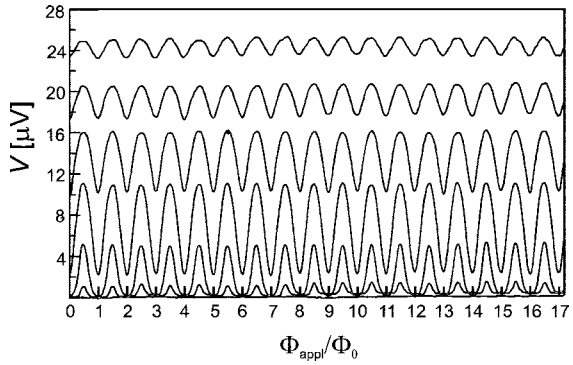

FIG. 1. Voltage modulation of a SQUID vs applied magnetic field at 37 K for different values of the bias current.

Typically, the current-voltage characteristics are nonhysteretic above 15 K. Hysteresis appears for some SQUIDs below this temperature and is believed to be of thermal nature. The typical critical current of a SQUID with two parallel 140-nm-wide bridges at $T=4.2$ K is measured to be 14 mA. With an estimated bridge cross section of 140×100 nm^2 this results in an exceptionally high critical current density of $J_c=5\times10^7$ A/cm^2, which indicates that the film quality in the bridges is good. The critical current density is still below the MgB_2 depairing current density, due to the onset of moving flux quanta that are released from their pinning sites (typically at the sides of a nanobridge) when the current becomes large.

The voltage across the SQUID under constant current bias is modulated by an applied magnetic field, as shown in Fig. 1 at 37 K. The modulation is stable and shows no drift over a large number of periods. The period of the voltage modulation versus magnetic field is estimated to be 1.6 μT. The effective SQUID area $A_{\mathrm{eff}}=\Phi_0/B_{\mathrm{ext}}$, is then estimated to be about 1.3×10^3 μm^2, where $\Phi_0=2.07\times10^{15}$ Tm^2. This is well in accordance with the actual SQUID dimensions (20×20 μm^2 hole in a 40×40 μm^2 washer), taking flux focusing by the superconducting washer into account. The SQUID inductance is estimated to be 48 pH. A suitable magnitude of the voltage modulation of 8 μV was observed at 37 K (Fig. 1). Voltage modulation was even observed up to 38.8 K, remarkably close to the material's bulk superconducting transition temperature, which stands in contrast to most high-T_c SQUIDs.

The SQUID modulation, as well as the large critical current densities of the nanobridges, shows that high-quality superconducting properties can be obtained when the nanobridge is likely to be contained within a single grain. The consequent step now is to investigate what field sensitivity can be obtained from these SQUIDs in a magnetometer configuration.

An inductively shunted magnetometer was designed as depicted in Fig. 2. The inductive shunt enhances the effective SQUID area, while keeping its inductance small. The effective sensing area A_{eff} of the magnetometer can be expressed as $A_{\mathrm{eff}}=(L_c/L_P)\cdot A_P$.[11] Here, L_c is the coupling part of the small SQUID loop inductance, $L_P=2.6$ nH is the inductance of the large pickup loop, with A_P being its effective pickup area. L_c is composed of a geometrical inductance and a kinetic inductance. Taking into account that the flux induced by the current I_p covers 80% of the area enclosed by the striplines [Fig. 2(b)], L_c is 0.8 times the small SQUID inductance, L_{SQ}. The geometrical part of L_{SQ} is estimated to be 37 pH, while the kinetic inductance of the SQUID striplines is $L_{\mathrm{SQ,kin}}=\mu_0\lambda(\ell/w)\coth(d/2\lambda)$, where $d=100$ nm, and ℓ and w are measured to be 51 and 6 μm, respectively. $L_{\mathrm{SQ,kin}}$ depends on the magnetic field penetration depth λ. The effective area is, therefore, a function of temperature. Five SQUIDs can be coupled to the same inductive shunt [Fig. 2(a)]. In the striplines, 100-nm-wide nanobridges were fabricated [Fig. 2(b)]. The device is based on a film deposited with 150 sccm B_2H_6 flow on a 5×5 mm^2 SiC substrate.

The measured voltage modulation of the magnetometer as a function of magnetic field under constant bias current is maximum 6 μV in the temperature range of 32–35 K. The measured voltage modulation as a function of temperature is shown in the inset of Fig. 3. The behavior is governed by the temperature dependence of the critical current as well as the SQUID inductance.

The period of the voltage modulation is indeed measured to be temperature dependent. The resulting temperature dependence of A_{eff} (see Fig. 3) allows us to obtain the penetration depth in MgB_2 as a function of temperature. Golubov *et al.*[12] obtained a two-band model for the MgB_2 penetration depth as a function of transport orientation and amount of impurities. We find that the temperature dependence of the effective area can be very well fitted with the two-band model in the clean limit with transport currents in the crystallographic *a-b* plane, whereas the Bardeen–Cooper–Schrieffer (BCS) model results in a much poorer fit. The same conclusion holds for the critical current as function of temperature. For a rounded bridge edge, as is the case here, the critical current is expected to be proportional to the product of λ^{-2} and ξ^{-1}. Given the temperature dependence for λ from the two-band model[12] and the experimental fit for the coherence length $\xi\sim(1-T/T_C)^{0.59}$ in the *a-b* plane in the clean limit,[13] the measured I_c vs T dependence can again be very well fitted as shown in Fig. 4. These findings support our assumption that transport occurs in crystalline MgB_2 and

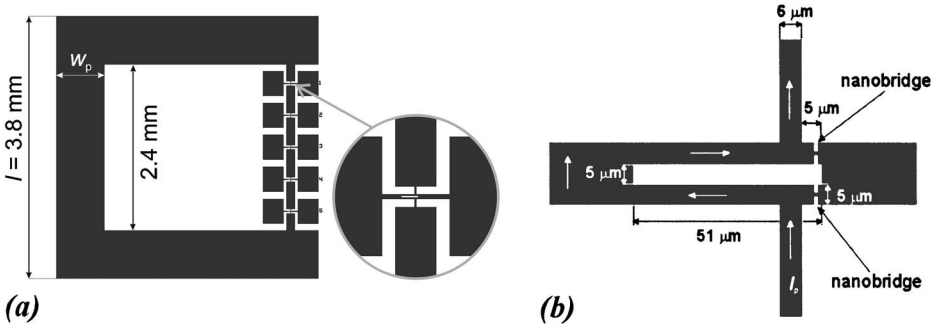

FIG. 2. The design of an inductively shunted magnetometer. (a) The design of the whole magnetometer with a magnification of the striplines; (b) including their dimensions and position of the nanobridges. I_p denotes the screening current, i.e., the current induced by the applied magnetic field.

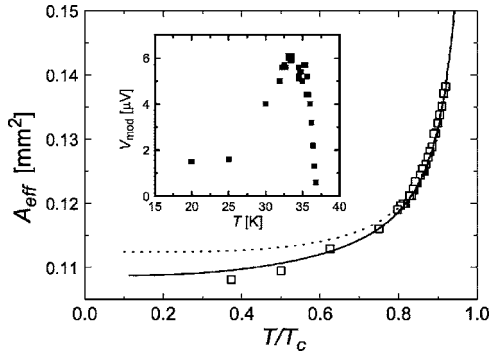

FIG. 3. Effective magnetometer area as function of temperature. The solid line is the theoretical expectation for $A_{\mathrm{eff}}(T)$ when using a two-band model for the MgB_2 penetration depth in the clean limit for transport in the crystallographic $a-b$ plane, with $\lambda(0)=62$ nm. The dotted line is the theoretical expectation when using a BCS model for the penetration depth and $\lambda(0)=110$ nm. The inset shows the maximum voltage modulation as a function of temperature.

furthermore indicate the absence of major impurity scattering within the grains. The $\lambda(0)$ value of 62 nm that is found from the fitting is smaller than previously reported when measured over larger film areas, but much closer to theoretical expectations.[12]

The noise spectrum of the magnetometer is determined using a flux-locked loop. For $T=35$ K, the voltage modulation was maximum and the measured noise spectrum is shown in Fig. 5 as a function of the frequency ν. The white noise level is 76 $\mu\Phi_0$ Hz$^{-1/2}$ and below 1 Hz, the noise appears with a magnitude proportional to $1/\nu$.[2] The effective magnetic field noise $S_B^{1/2}(\nu)=S_\phi^{1/2}(\nu)/A_{\mathrm{eff}}=1$ pT Hz$^{-1/2}$. Despite the fact that single-crystalline MgB_2 has weaker flux-pinning properties than polycrystalline samples,[14] the obtained noise value indicates that this does not pose any problems. The obtained magnetometer noise value is promising for a device that has not yet been optimized. For high temperature semiconductor magnetometers, lower noise values were reported (~20–100 fT Hz$^{-1/2}$ at 1 Hz at 77 K, see, e.g., Refs. 11 and 15), but these were fabricated on larger samples (1–4 cm^2). Using larger MgB_2 samples, the magnetic field noise level in inductively shunted dc SQUIDs is expected to be reduced as well. The presented work shows that an adult magnetocardiogram mesurement is already feasible at this stage.

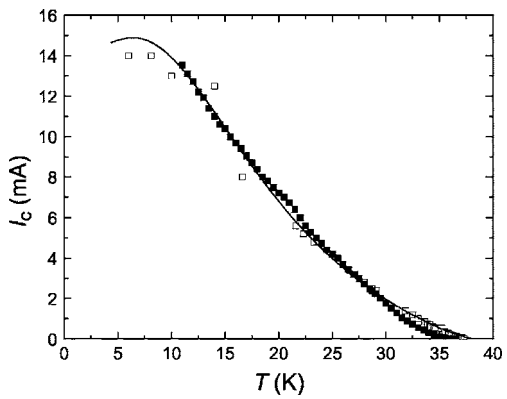

FIG. 4. Temperature dependence of the critical current in a MgB_2 nanobridge of 100 nm width (■), scaled up by a factor of 4, and 140 nm width (○). The solid line shows the (nonmonotonous) fit of a two-band model.

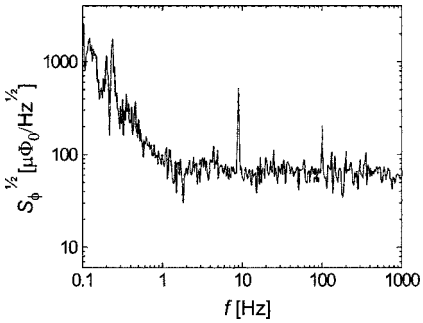

FIG. 5. Flux noise spectrum of the magnetometer at 35 K.

In conclusion, magnetic sensing above 35 K is shown to be feasible with MgB_2. Nanoconstrictions were realized in epitaxial HPCVD MgB_2 films within the single-crystalline grains of the material. The 100-nm-wide nanobridges show a high critical current density of 5×10^7 A/cm^2 at 4.2 K and SQUID modulation was observed up to 38.8 K, remarkably close to the transition temperature of the film. An inductively shunted magnetometer was realized with a field-noise level of 1 pT Hz$^{-1/2}$ down to 1 Hz. The transport properties of the magnetometer are governed by the two-band nature of superconductivity, which is found not to hamper the successful development of MgB_2 SQUIDs.

This work is supported by the Netherlands Organization for Scientific Research (NWO) and the Dutch Foundation for Research on Matter (FOM), and is part of the MESA+ Strategic Orientation on Materials Science of Interfaces. D.M. acknowledges the hospitality during her stay at PSU. The work at Penn State is supported in part by ONR under Grant Nos. N00014-00-1-0294 (X.X.X.) and N0014-01-1-0006 (J.M.R.), and by NSF under Grant Nos. DMR-0306746 (X.X.X. and J.M.R.), and DMR-0405502 (Q.L.).

[1] A. Brinkman, D. Veldhuis, D. Mijatovic, G. Rijnders, D. H. A. Blank, H. Hilgenkamp, and H. Rogalla, Appl. Phys. Lett. **79**, 2420 (2001).
[2] Y. Zhang, D. Kinion, J. Chen, J. Clarke, D. G. Hinks, and G. W. Crabtree, Appl. Phys. Lett. **79**, 3995 (2001).
[3] G. Burnell, D.-J. Kang, D. A. Ansell, H.-N. Lee, S.-H. Moon, E. J. Tarte, and M. G. Blamire, Appl. Phys. Lett. **81**, 102 (2002).
[4] Physica C **385**, issue 1-2 (2003) (Special issue on MgB_2).
[5] X. H. Zeng, A. V. Pogrebnyakov, A. Kotcharov, J. E. Jones, X. X. Xi, E. M. Lysczek, J. M. Redwing, S. Y. Xu, J. Lettieri, D. G. Schlom, W. Tian, X. Q. Pan, and Z. K. Liu, Nat. Mater. **1**, 35 (2002).
[6] D. C. Larbalestier, L. D. Cooley, M. O. Rikel, A. A. Polyanskii, J. Jiang, S. Patnaik, X. Y. Cai, D. M. Feldmann, A. Gurevich, A. A. Squitieri, M. T. Naus, C. B. Eom, E. E. Hellstrom, R. J. Cava, K. A. Regan, N. Rogado, M. A. Hayward, T. He, J. S. Slusky, P. Khalifah, K. Inumaru, and M. Haas, Nature (London) **410**, 186 (2001).
[7] D. K. Finnemore, J. E. Ostenson, S. L. Bud'ko, G. Lapertot, and P. C. Canfield, Phys. Rev. Lett. **86**, 2420 (2001).
[8] D. Mijatovic, Ph.D. thesis, University of Twente, The Netherlands (2004).
[9] H. Y. Zhai, H. M. Christen, L. Zhang, M. Paranthaman, P. H. Fleming, and D. H. Lowndes, Supercond. Sci. Technol. **14**, 425 (2001).
[10] D. K. Aswal, K. P. Muthe, A. Singh, S. Sen, K. Shah, L. C. Gupta, S. K. Gupta and V. C. Sahni, Physica C **363**, 208 (2001).
[11] D. Koelle, A. H. Miklich, F. Ludwig, E. Dantsker, D. T. Nemeth, and J. Clarke, Appl. Phys. Lett. **63**, 2271 (1993).
[12] A. A. Golubov, A. Brinkman, O. V. Dolgov, J. Kortus, and O. Jepsen, Phys. Rev. B **66**, 054524 (2002).
[13] S. Y. Xu, Q. Li, and X. X. Xi, Experimental dependence of the coherence length measured in Penn State University (private communication).
[14] Z. X. Shi, A. K. Pradhan, M. Tokunaga, K. Yamazaki, T. Tamegai, Y. Takano, K. Togano, H. Kito, and H. Ihara, Phys. Rev. B **68**, 104514 (2003).
[15] R. Cantor, L. P. Lee, M. Teepe, V. Vinetskiy and J. Longo, IEEE Trans. Appl. Supercond. **5**, 2927 (1995).